Designed Nanoparticle-Mesoporous Multilayer Nanocomposites as Tunable Plasmonic-Photonic Architectures for Electromagnetic Field Enhancement

Rodrigo Martínez Gazoni,[1] Martín G. Bellino,[1,2] M. Cecilia Fuertes,[1]Gustavo Giménez,[3]Galo J.A.A. Soler-Illia,[4,5*] María Luz Martínez Ricci[4,6*]

[1] *Gerencia Química, Centro Atómico Constituyentes, Comisión Nacional de Energía Atómica, Avenida General Paz 1499, B1428KNA, San Martín, Argentina*

[2]*Departamento de Micro y Nanotecnología, Centro Atómico Constituyentes, Comisión Nacional de Energía Atómica, Avenida General Paz 1499, B1428KNA, San Martín, Argentina*

[3]*CNMB, Instituto Nacional de Tecnología Industrial, Avenida General Paz 5445, B1650WAB, San Martín, Argentina*

[4]*DQIAQF, Facultad de Ciencias Exactas y Naturales, Universidad de Buenos Aires, Ciudad Universitaria, Pab. II, C1428EHA, Ciudad Autónoma de Buenos Aires, Argentina*

[5]*Instituto de Nanosistemas, Universidad Nacional de General San Martín, Av. 25 de Mayo y Francia, 1650, San Martín, Argentina*

[6]*INQUIMAE, Facultad de Ciencias Exactas y Naturales, Universidad de Buenos Aires, Ciudad Universitaria, Pab. II, C1428EHA, Ciudad Autónoma de Buenos Aires, Argentina*

Electronic Supplementary Information

1- Experimental Details

Monolayer Synthesis and Detailed Optical Characterization

Mesoporous Thin Films (MTF): SiO_2 and TiO_2 mesoporous monolayer films on Si substrates were synthesized by dip coating. Silica solutions were composed of TEOS:EtOH:H_2O:HCl:CTAB = 1:40:10:0.26:0.05 molar ratio, where TEOS (tetraethyl orthosilicate, Merck) is the Si precursor and CTAB (cetyltrimethylammonium bromide, Aldrich) is the surfactant. These solutions were aged during 72 h at room temperature under stirring to obtain an ordered 3D-hexagonal mesostructure.[1] The titania solution was prepared from $TiCl_4$ (Aldrich) precursor. Stock solutions were prepared by slowly dripping $TiCl_4$ (0.05 mol) in 100g absolute ethanol, at 0ºC. To obtain 20g of this solution, 0.7g Pluronics®F127 ($HO(CH_2CH_2O)_{106}(CH_2CH(CH_3)_O)_{70}$-$(CH_2CH_2O)_{106}OH$, Aldrich) templating agent was added. Finally, 1.8g water (Milli-Q quality (18 MΩ.cm) was added. All reactants were provided by Aldrich.

Mesoporous Photonic Crystals (MPC) were produced by successive deposition of alternate titania and silica mesoporous layers. Films were deposited by dip-coating on silicon

substrates, at a withdrawal speed of 1 mm.sec^{-1}. Once extracted from the solution, films were submitted to 50% relative humidity (RH) for 30 min and then exposed to two stabilization thermal stages of 60ºC and 130ºC for 30 min each. Finally, the organic template was eliminated in a calcination stage of 350ºC for 2h. Using this synthesis strategy, transparent, crack-free and homogeneous mesoporous thin films were obtained. To produce multilayered structures, a step-wise process was fulfilled: after each dip-coating step, films were submitted to ageing in 50% RH chambers for 30min, followed by thermal stages of 60ºC and 130ºC for 30 min each, and a final thermal treatment at 200ºC for 2h. This last step is meant to consolidate the inorganic framework without eliminating the template, and so next film can be dip-coated on the previously stabilized one.[2] This process was repeated for each new layer until the whole multilayered structure wasfinished. The MPCs obtained (up to 8 layers) were finally exposed to a calcination step of 350ºC for 2h, in order to eliminate the template and to open the mesopore structure. To obtain MPCs with thinner layers (60-70nm each), 1:40 ethanol diluted solutions were prepared; each SiO_2 and TiO_2 layers were synthesized using the diluted solutions and following the same procedures detailed above.

Non-periodic structures that reproduced the total number of layers and the total thicknesses found in the MPCs were also designed and synthesized. These systems, labeled *stacks*, present no periodicity. Stacks were produced by dip-coating successively TiO_2 layers over successive SiO_2 layers (system labeled sSiTi); the thickness of each layer was either 70nm or 110nm depending on the desired final structure.

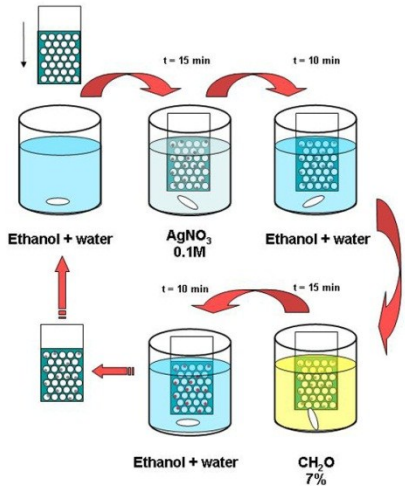

Scheme 1-ESI: Schematic illustration of the different steps involved in the Ag NPs infiltration process

Infiltration of MTF with Ag NPs: The infiltration method to synthesize Ag NPs inside the pore systems of the TiO_2 layers is presented in Scheme-ESI 1, and was adapted from reference [3]. MPC samples were first thoroughly washed in an ethanol/water solution in order to eliminate eventual pore obstructions and to improve its accessibility. After drying, films were placed for 15min in a 0.1M $AgNO_3$ solution under continuous stirring; these conditions assist the Ag^+ adsorption on the pore surface. The films were rinsed and dried again in order to eliminate any unabsorbed ions. Finally, the films with adsorbed Ag^+ were immersed in a

7% HCHO solution at continuous stirring for 10min, leading to the formation of metallic Ag nanoparticles inside the pores. One final rinse stage eliminates any residual Ag NP from the sample surface.

Modeling of the film optical properties: UV-Vis spectroscopic ellipsometry was employed to measure the refractive index and thickness of the samples.

- *MTF:* Cauchy model was employed to describe the optical response of SiO_2[4, 5]:

$$n(\lambda) = A_c + \frac{B_c}{\lambda^2}, \qquad \text{(1-ESI)}$$

while a Cauchy–Lorentz model was used for TiO_2 samples[6]:

$$n(\lambda) = \left[\left(A_c + \frac{B_c}{\lambda^2}\right)^2 + \left(A_l \frac{\lambda^2(\lambda^2 - \lambda_0^2)}{\left[(\lambda^2 - \lambda_0^2)^2 + \lambda^2\gamma_l^2\right]}\right) + i\left(A_l \frac{\lambda^3\gamma_l}{\left[(\lambda^2 - \lambda_0^2)^2 + \lambda^2\gamma_l^2\right]}\right)\right]^{1/2}, \qquad \text{(2-ESI)}$$

where n is the complex refractive index of the medium, λ is the incident wavelength. A_c, B_c are the Cauchy parameters to be adjusted by the ellipsometric measurements, as well as A_l, λ_0, γ_l which correspond to the Lorentz model. Best fit of the defined parameters for empty films, are detailed in Table 1.

The Cauchy/ Cauchy-Lorentz best fit parameters obtained at 25°C and 50% RH for both SiO_2 and TiO_2 MTFs are exhibited in the first two rows of Table 1. A range of values is given for each parameter as a result from ellipsometric measurements on several SiO_2 and TiO_2 mesoporous monolayers and bilayers.

- *Ag@TiO₂*:Ellipsometric spectroscopy measurements were also performed on samples filled with Ag NPs. To characterize Ag@TiO_2–F127 samples a new Lorentz term has to be added to the Cauchy/Lorentz equation (2) to account for the LSPR absorbance as shown in eq. (3).

$$n(\lambda) = \left[\left(A_c + \frac{B_c}{\lambda^2}\right)^2 + \left(A_l \frac{\lambda^2\left(\lambda^2 - \lambda_0^2\right)}{\left[\left(\lambda^2 - \lambda_0^2\right)^2 + \lambda^2\gamma_l^2\right]}\right) + i\left(A_l \frac{\lambda^3\gamma_l}{\left[\left(\lambda^2 - \lambda_0^2\right)^2 + \lambda^2\gamma_l^2\right]}\right) + \right. \qquad \text{(3-ESI)}$$
$$\left. + \left(A_{lp} \frac{\lambda^2(\lambda^2 - \lambda_{0p}^2)}{\left[(\lambda^2 - \lambda_{0p}^2)^2 + \lambda^2\gamma_{lp}^2\right]}\right) + i\left(A_{lp} \frac{\lambda^3\gamma_{lp}}{\left[(\lambda^2 - \lambda_{0p}^2)^2 + \lambda^2\gamma_{lp}^2\right]}\right)\right]^{1/2},$$

where $A_{lp}, \lambda_{lp}, \gamma_{lp}$ are the Lorentz model parameters to be defined by the ellipsometric measurement to consider the plasmon absorbance. At 25°C and 50% RH, the obtained ellipsometric parameters range for Ag@TiO_2–F127 slabs is shown in the last row of Table

1-ESI.

Material	A_c	B_c [nm^2]	A_l	λ_0 [nm]	γ_l [nm]	A_{lp}	λ_{0p} [nm]	γ_{lp} [nm]
SiO_2-CTAB	1.2 – 1.22	1.5×10^3 – 4×10^3	-	-	-	-	-	-
TiO_2-F127	1.4 – 1.45	2×10^4 – 5×10^4	0.17 – 0.3	280 - 288	35 - 60			
Ag@TiO_2-F127	1.45 – 1.55	2×10^4 – 4×10^4	0.3 – 0.45	280 - 288	35 – 60	0.1-0.4	445-455	130-160

Table 1-ESI. Ellipsometric parameters obtained from SiO_2-CTAB and TiO_2-F127 mesoporous monolayers and bilayers before and after Ag infiltration

The absorbance spectra of an Ag@TiO_2 thin film is shown in Figure 1-ESI. Typical plasmon peak is observed centered at 450nm with a FWHM of 100nm aprox.

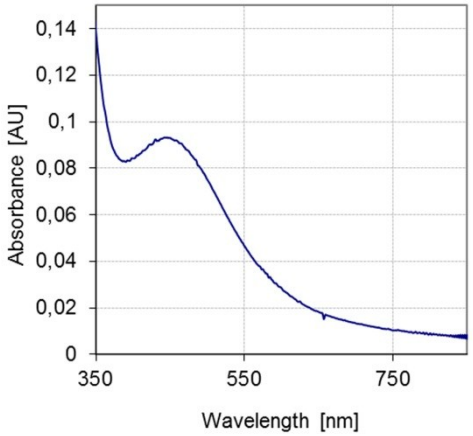

Figure 1-ESI: UV-Vis spectra of the MTF TiO_2-F127on silicon substrate after 15min of Aginfiltration

*Detailed modeling of the PC structure:*The SiO_2-TiO_2unit celloptical parameters were obtained by fitting theCauchy or Cauchy–Lorentz models to the experimental data obtained from ellipsometry measurements conducted on monolayers of SiO_2 and TiO_2, respectively.These parameters werethe input for the PCs´ numerical models employed both to determine the layers´ thicknesses required to synthesize a multilayer with the required optical response (photonic band gap spectral position) and to calculate the density field distribution within the structures. The same procedure was followed to determine the optical response of each layer and the complete photonic crystal when pores were filled with Ag NPs.

In order to model the optical response and the EM density field distribution of the multilayer structure, a transference matrix[7](*T-Matrix*) method was applied.

A multilayer structure comprises a periodic succession of layers stacked in z-direction as shown in Figure 2-ESI. In each period or *unit cell*,layers present different electric permittivity$\varepsilon_j(\lambda)$(where $\varepsilon_j(\lambda) = [n_j(\lambda)]^2$) and each interface is placed in z_j position. The incident field is described by a plane wave of wavevector $k = (k_x, 0, k_z)$where $k_x = \frac{2\pi}{\lambda}\sqrt{\varepsilon_{inc}}\sin\theta_i = \alpha_0$ (optical media is being considered so the magnetic permeability $\mu = 1$ for all layers); being ε_{inc} the electric permittivity of the incident medium andθ_i the angle of incidence. The z-component of $k$at each layer is then defined as:

$$k_{z,j}^2 = \frac{\omega^2}{c^2}\varepsilon_j - \alpha_0^2;$$

where ω is the wave frequency and c the light velocity.

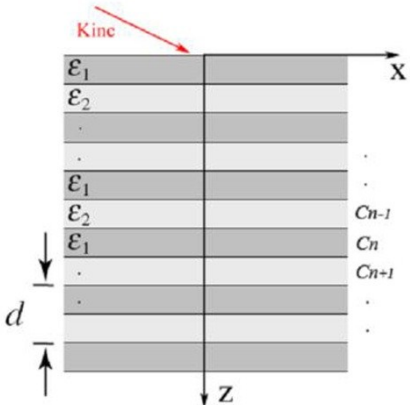

Figure 2-ESI: Multilayer scheme of unit cell composed of two layers of different refractive

In this work,normal incidence wasconsidered ($\theta_i = 0$), and consequently no polarization distinction is necessary and the electric field $E(z)$ at each $j$layer can be written as a superposition of propagating and anti-propagating waves as detailed in eq. (4):

$$E_j(z_j) = A_j e^{ik_{z,j}z_j} + B_j e^{-ik_{z,j}z_j}, \qquad (4\text{-ESI})$$

Applying the corresponding boundary conditions at each z_j, it is possible to use a matrix representation at each interface as given in eq. (5):

$$\underbrace{\begin{pmatrix} e^{-ik_{z,j}z_j} & e^{ik_{z,j}z_j} \\ -\frac{k_{z,j}}{\varepsilon_j}e^{-ik_{z,j}z_j} & \frac{k_{z,j}}{\varepsilon_j}e^{-ik_{z,j}z_j} \end{pmatrix}}_{M_j(z_j)} \begin{pmatrix} A_j \\ B_j \end{pmatrix} = \underbrace{\begin{pmatrix} e^{-ik_{z,j-1}z_j} & e^{ik_{z,j-1}z_j} \\ -\frac{k_{z,j-1}}{\varepsilon_{j-1}}e^{-ik_{z,j-1}z_j} & \frac{k_{z,j-1}}{\varepsilon_{j-1}}e^{-ik_{z,j-1}z_j} \end{pmatrix}}_{M_{j-1}(z_j)} \begin{pmatrix} A_{j-1} \\ B_{j-1} \end{pmatrix}, \qquad (5\text{-ESI})$$

where $M_j(z_j)$ represents the matrix of the j layer at the j interface, which links with the $j-1$ layer at the same j interface -matrix $M_{j-1}(z_j)$-.

Repeating this set of equations for each interface, it is possible to express the field amplitudes of the j layer as a function of all the precedent matrices,

$$\begin{pmatrix} A_j \\ B_j \end{pmatrix} = [M_j(z_j)]^{-1} M_{j-1}(z_j) \begin{pmatrix} A_{j-1} \\ B_{j-1} \end{pmatrix} =$$

$$= \left[M_j(z_j)\right]^{-1} M_{j-1}(z_j) \ldots\ldots\ldots\ldots \left[M_2(z_2)\right]^{-1} M_1(z_2)\begin{pmatrix} A_1 \\ B_1 \end{pmatrix} =$$

$$= M\begin{pmatrix} A_1 \\ B_1 \end{pmatrix}, \qquad \text{(6-ESI)}$$

where M is defined as the *transfer matrix*between layers j and 1.

Following the described procedure it is possible to define the Reflectivity(R) and Transmission (T) coefficientsof the multilayered structure defined as expressed in eqs. (7a-ESI) - (7b-ESI):

$$R(\lambda) = \left|\frac{B_1}{A_1}\right|^2 = \left|\frac{M_{21}}{M_{11}}\right|^2, \qquad \text{(7a-ESI)}$$

$$T(\lambda) = \left|\frac{A_j}{A_1}\right|^2 = \left|M_{11} + M_{12}\frac{M_{21}}{M_{11}}\right|^2, \qquad \text{(7b-ESI)}$$

where A_1 is the amplitude of the incident field and M_{kl} (with $k,l = 1, 2$) are the components of the transfer matrix M. It is important to remark that the *T-Matrix* method allows to obtain the EM field intensity map inside the structure recovering from eq. (6-ESI) each one of the field amplitudes at each layer.

Figure3-ESI shows the modeled transmittance spectrafor both designed PCs together with the measured spectrum of a TiO_2 monolayer with Ag NP adsorbedinside its pores. It is possible to observe the correct matching location of the LSPR with the corresponding BG edges of both designed structures (region denoted with a shaded strip).

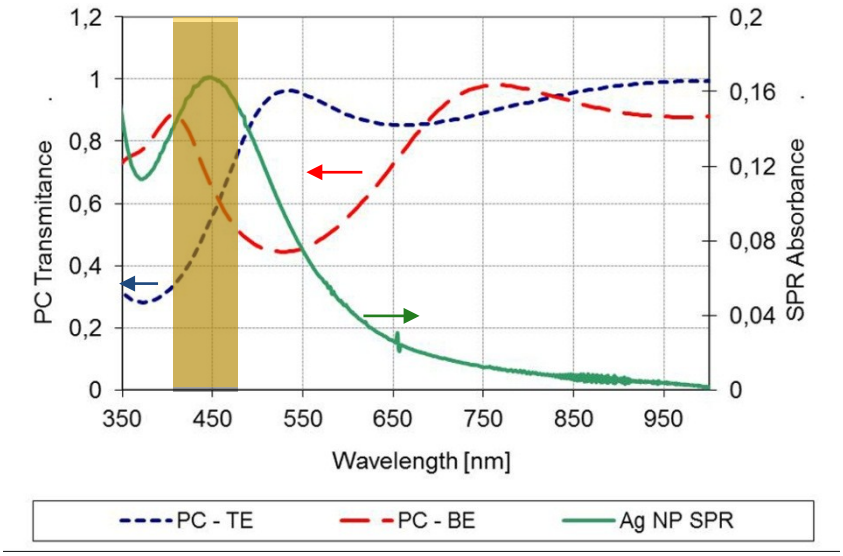

Figure 3-ESI: Designed PC structures (*PC-BE* and *PC-TE*) transmittance. Good accordance of the corresponding edge with the Ag NP SPR position is observable.

Despite the success in tuning the MPC so that either the top edge band or the bottom edge band of its PBG match the adsorbed NP's SPR; models also showed that when considering the presence of Ag NPs insidethe TiO_2 layers (using the parameters present in Table 1-ESI), the PBG widens and flattens. Consequently, these effects had to be taken into account for the design and synthesis of the final crystals in order to keep the top or bottom edges matching the LSPR location once the NPs are grown inside the TiO_2 layer pores. To assure this, final PCs were designed with the corresponding PBG slightly shifted from the required condition so as to get its final location once the NP synthesis is accomplished. The final PCs' layers thicknesses where 70nm and 110nm for the PC-BE and PC-TE structures, respectively.

*Photonic Crystals Reflectance:*Figures4a-ESI and 4c-ESI present the modeled reflectance for the tunedmultilayer structures and the corresponding measured reflectivity of the samples synthesized using the parameters obtained from the models. Figs. 4b-ESI and d-ESI show respective SEM images of the structures exhibiting excellent homogeneity along each layer of the composed structure.

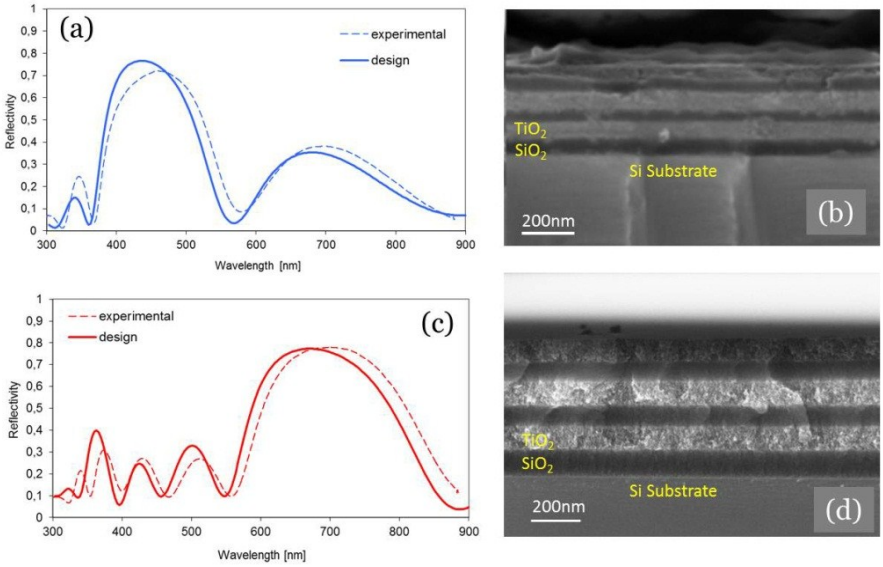

Figure 4-ESI: Modeled (designed, prior to the synthesis), measured reflectance spectra and cross-section SEM images of 6-layered PC (SiO_2-CTAB/TiO_2-F127).

Fig. 4-ESI shows that the reflectance spectra of both synthesized structures are in very good agreement with the designed ones. Only 10 nm difference can be noticed in the PBG location between the designed and the obtained crystals while the amplitude discrepancies are among 5 - 15%.These small differences can be originated in the variability of the synthesis technique as well as differences in the reflectance measurements due to the ambient humidity. The synthesis parameters for each PC (obtained from modeling and from experimental data) are shown in Table 2-ESI.

Label	Layer width	PBG centre	Sol dilution	Dip coater speed	Total PC synthesis time
PC-TE	~ 70nm	420 nm	1: 0.4 ethanol	1 mm/s	1-2 days
PC-BE	~ 110nm	660 nm	---	1.2 mm/s	1-2 days

Table 2-ESI: Synthesis parameters for the designed PCs

The parameters used to design the PCs were obtained from the characterization of single and bi-layered structures. Consequently, results displayed in Fig. 4-ESI validate our model-synthesis procedure, allowing us to design and obtain specific PCs with accurate PBG selectivity.

Ag particle statistical analysis: Figs 5-ESIdisplays the PSD obtained fromnanoparticle size analysis conducted on different STEM images of Figure 5. Fig. 5a-ESI relates to low Ag-loading of the MPC, which corresponds to 45min infiltration of $AgNO_3$ followed by 20min reduction with COH_2 while Fig. 5b-ESI relates to high Ag-loading of the multilayer, obtained after 3h infiltration of $AgNO_3$ followed by 1.5h reduction with COH_2. Statistical analysis reports an average diameter of(4.9±0.8)nm for case (a)and (6.7±0.7)nm for case (b); which infers not only a nucleation mechanism inside each pore but also a growth one.

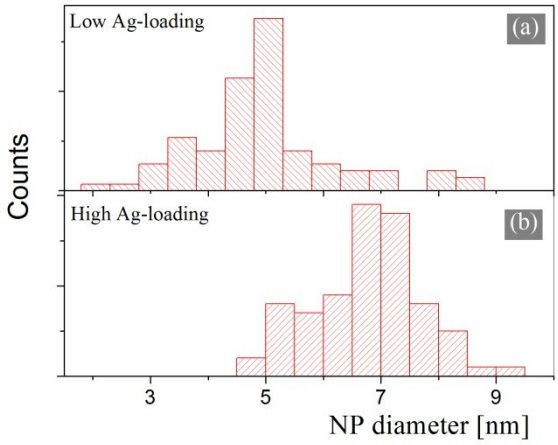

Figure 5-ESI: PSD study of nanoparticle size from STEM images corresponding to (a) Figure 5b - MPC after 45min infiltration of $AgNO_3$ followed by 20min reduction with COH_2(b) Figure 5c - MPC after 3h $AgNO_3$ infiltration followed by 1.5h reduction with COH_2.

*Stacks Reflectance:*Figs.6a-ESI and c-ESI show the reflectivity spectra of the synthesized stacks, displaying the experimental data obtained together with the numerical modeling results exhibiting very good accordance between them. The reflectivity shows the absence of band gaps as a consequence of the lack of periodicity, in contrast to the results observedfor the periodic structures presented in Figure 4-ESI.

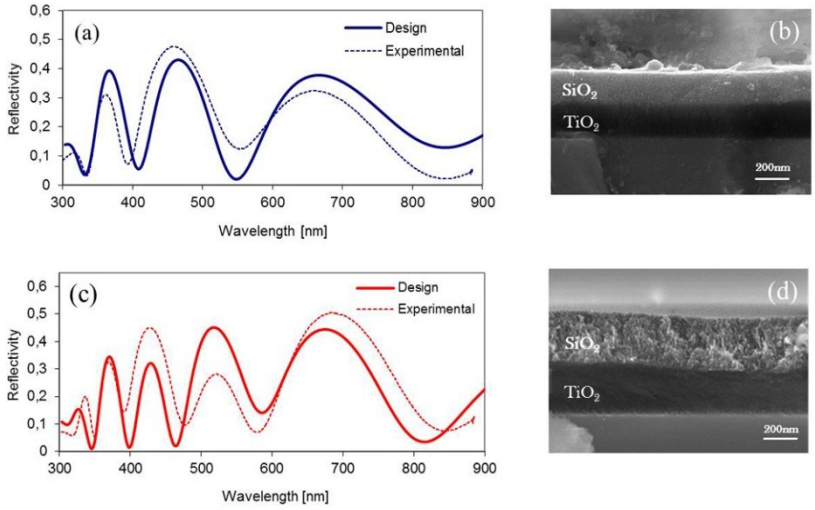

Figure 6-ESI: (a) and (c) Reflectance spectra for stacks. No PBG is observable. (b) and (d) Cross-section SEM images of the synthesized stacks.

1. D. Grosso, A. R. Balkenende, P. A. Albouy, A. Ayral, H. Amenitsch and F. Babonneau, *Chemistry of Materials*, 2001, **13**, 1848-1856.
2. M. C. Fuertes, F. J. López-Alcaraz, M. C. Marchi, H. E. Troiani, V. Luca, H. Míguez and G. d. A. Soler-Illia, *Advanced Functional Materials*, 2007, **17**, 1247-1254.
3. M. C. Fuertes, M. Marchena, M. C. Marchi, A. Wolosiuk and G. J. A. A. Soler-Illia, *Small*, 2009, **5**, 272-280.
4. A. Fischereder, M. L. Martinez-Ricci, A. Wolosiuk, W. Haas, F. Hofer, G. Trimmel and G. J. Soler-Illia, *Chemistry of Materials*, 2012, **24**, 1837-1845.
5. H. G. Tompkins and W. A. McGahan, *Spectroscopic ellipsometry and reflectometry: a user's guide*, Wiley New York, 1999.
6. A. B. Djurišic and E. H. Li, *Applied optics*, 1998, **37**, 5291-5297.
7. P. Yeh, A. Yariv and C.-S. Hong, *JOSA*, 1977, **67**, 423-438.